JSHC
Japan Society of
Histochemistry and Cytochemistry
Established 1959

Acta Histochem. Cytochem. 48 (2): 61–68, 2015
doi: 10.1267/ahc.14065

SCGB3A2 Inhibits Acrolein-Induced Apoptosis through Decreased p53 Phosphorylation

Reiko Kurotani[1], Reika Shima[1], Yuki Miyano[1], Satoshi Sakahara[1], Yoshie Matsumoto[1], Yoko Shibata[2], Hiroyuki Abe[1] and Shioko Kimura[3]

[1]Biochemical Engineering, Graduate School of Science and Engineering, Yamagata University, Yonezawa, Yamagata 992–8510, Japan, [2]Department of Cardiology, Pulmonology, and Nephrology, Yamagata University School of Medicine, 2–2–2 Iida-Nishi, Yamagata 990–9585, Japan and [3]Laboratory of Metabolism, National Cancer Institute, National Institutes of Health, Bethesda, MD 20892

Received December 12, 2014; accepted March 21, 2015; published online April 24, 2015

Chronic obstructive pulmonary disease (COPD), a major global health problem with increasing morbidity and mortality rates, is anticipated to become the third leading cause of death worldwide by 2020. COPD arises from exposure to cigarette smoke. Acrolein, which is contained in cigarette smoke, is the most important risk factor for COPD. It causes lung injury through altering apoptosis and causes inflammation by augmenting p53 phosphorylation and producing reactive oxygen species (ROS). Secretoglobin (SCGB) 3A2, a secretory protein predominantly present in the epithelial cells of the lungs and trachea, is a cytokine-like small molecule having anti-inflammatory, antifibrotic, and growth factor activities. In this study, the effect of SCGB3A2 on acrolein-related apoptosis was investigated using the mouse fibroblast cell line MLg as the first step in determining the possible therapeutic value of SCGB3A2 in COPD. Acrolein increased the production of ROS and phosphorylation of p53 and induced apoptosis in MLg cells. While the extent of ROS production induced by acrolein was not affected by SCGB3A2, p53 phosphorylation was significantly decreased by SCGB3A2. These results demonstrate that SCGB3A2 inhibited acrolein-induced apoptosis through decreased p53 phosphorylation, not altered ROS levels.

Key words: secretoglobin (SCGB) 3A2, chronic obstructive pulmonary disease (COPD), apoptosis, acrolein, p53

I. Introduction

Chronic obstructive pulmonary disease (COPD) is a major global health problem with increasing morbidity and mortality rates. It is anticipated that COPD will become the third leading cause of death worldwide by 2020 [10]. COPD is associated with severe impairment in quality of life, disability, and increased healthcare costs [2, 17, 37]. COPD, an obstructive airway disease involving chronic inflammation of the respiratory tract caused by smoke from cigarettes and biomass fuels [16], is associated with emphysema [3, 18, 26, 41]. The proposed pathogenesis of COPD includes the proteinase–antiproteinase hypothesis, immunological mechanisms, oxidant–antioxidant balance, systemic inflammation, apoptosis, and ineffective repair [49]. Further, excessive oxidative stress is noted in long-term cigarette smokers [33].

Although cigarette smoke contains numerous chemical components, acrolein (ACR), which is abundant in cigarette smoke, is thought to be the most important component of smoke condensate leading to COPD [4]. ACR inhibits cell signaling mediated by epidermal growth factor receptor, mitogen-activated protein kinase (MAPK), and mammalian target of rapamycin (mTOR). Inhibition of these signaling pathways alters the regulation of matrix metalloproteinases (MMPs), such as MMP-1, MMP-2,

Correspondence to: Reiko Kurotani, Ph.D., Biochemical Engineering, Faculty of Engineering, Yamagata University, Yonezawa, Yamagata 992–8510, Japan. E-mail: kurotanir@yz.yamagata-u.ac.jp

MMP-9, and MMP-14, as well as the regulation of a proteinase inhibitor, tissue inhibitor of MMP (TIMP) 3, *in vivo* and *in vitro*. The alteration results in unbalanced proteinase activation [14, 15, 19, 24]. Moreover, ACR can induce the accumulation of macrophages [7] and neutrophils [6] following the production of high levels of proinflammatory cytokines/chemokines and proteases, including neutrophil elastase. This accumulation may contribute to alveolar destruction, tissue injury, and remodeling in COPD [7, 11]. ACR is also a factor responsible for altering apoptosis and inflammation through increased levels of p53 phosphorylation and production of reactive oxygen species (ROS) in human lung cells [42]. ROS are mainly produced in mitochondria and can lead to cell injury, DNA damage, and apoptosis. Apoptosis is increased in the alveolar epithelial and endothelial cells of COPD patients and is considered to be an important aspect of COPD pathogenesis. Furthermore, p53 is an important factor in the induction of DNA damage and apoptosis; serum p53 antibodies are increased in heavy smokers [25, 29], and p53 expression is increased in the lungs of smokers with COPD [46].

Secretoglobin (SCGB) 3A2 is a member of the SCGB gene superfamily, which consists of cytokine-like secreted proteins of low molecular weight [20, 35, 36]. SCGB3A2 exhibits anti-inflammatory [9] and antifibrotic activities [23]. SCGB3A2 also exhibits growth factor activity, having the potential to regenerate epithelial cells in the lung [22]. Macrophage scavenger receptor with collagenous structure (MARCO), which is expressed in alveolar macrophages in the lung, was reported as a possible SCGB3A2 receptor [5]. We previously reported the possibility that an SCGB3A2-specific receptor different from MARCO is present in mouse fetal lung mesenchymal cells [22]. Thus, SCGB3A2 has the potential for improving respiratory diseases, including COPD; however, little is known about the biological and physiological roles of SCGB3A2 in COPD.

In this study, we investigated the effect of SCGB3A2 on ACR-induced apoptosis in an *in vitro* cell culture system as the first step toward understanding whether SCGB3A2 plays a role in COPD pathogenesis and to determine the potential use of SCGB3A2 in the treatment of COPD. The results demonstrate that SCGB3A2 inhibited ACR-induced apoptosis through decreased phosphorylation of p53 but not through the inhibition of ROS production.

II. Materials and Methods

Cell culture

The mouse lung fibroblast cell line MLg was obtained from the American Type Culture Collection (Manassas, VA, USA). Cells were cultured in Dulbecco's modified Eagle's medium (DMEM) supplemented with 10% fetal bovine serum (FBS) and penicillin-streptomycin mixed solution (Nacalai Tesque, Kyoto, Japan), at 37°C in 5% CO_2 and 95% air.

Fifty thousand cells were seeded into each well of an 8-well Lab Tek Chamber Glass Slide (Thermo Scientific, Yokohama, Japan) for the terminal transferase dUTP nick-end labeling (TUNEL) assay, the annexin V binding assay, ROS detection, and immunocytochemistry. The next day, cells were cultured with fresh media containing 0, 15, 30, and 60 μM ACR (C_3H_4O) (Tokyo Chemical Industry Co., LTD., Tokyo, Japan) for 30 min at 37°C. The ACR-containing media were replaced with fresh media containing 0 or 300 ng/ml SCGB3A2 and the cells were cultured for an additional 16 hr, before being subjected to immunocytochemical analyses. One million cells were seeded onto 60-mm-diameter dishes (Greiner Bio-One, Tokyo, Japan) for immunoblotting; 150 ng/ml SCGB3A2 was added to the culture media. SCGB3A2 was purified as previously reported [22].

Assessment of cell apoptosis

The TUNEL assay (DeadEnd™ Fluorometoric TUNEL System; Promega, Fitchburg, WI, USA) and the annexin V binding assay (Clonetech, Mountain View, CA, USA) were performed to assess the level of cell apoptosis. The TUNEL assay detects DNA fragmentation and annexin V bound to externalized phosphatidylserine on the outer surface of apoptotic cells. To perform the TUNEL assay, cells treated with ACR and/or SCGB3A2 were fixed with 4% paraformaldehyde (PFA) in phosphate buffer (PB) at room temperature (RT) for 15 min. Cells were then incubated in phosphate-buffered saline (PBS), pH 7.4, supplemented with 0.2% Triton X-100 (T-PBS) for 15 min at RT. Next, cells were incubated with recombinant terminal deoxynucleotidyl transferase (rTdT) incubation buffer, which includes Nucleotide Mix, rTdT enzyme, and Equilibration Buffer (EB), for 1 hr at 37°C in the dark, followed by incubation in EB for 10 min at RT, to label the nicked DNA with dUTP. The reactions were terminated by incubation in 2×SSC for 15 min at RT. Cell nuclei were stained with 300 nM 4',6-diamino-2-phenylindole (DAPI) (Life Technologies, Carlsbad, CA, USA) for 5 min in the dark at RT, washed in PBS 3 times, and finally mounted with CC/Mount™ (Diagnostic BioSystems, Pleasanton, CA, USA). Nicked DNA was detected with a BX51 fluorescence microscope (Olympus, Tokyo, Japan). To perform the annexin V binding assay, the cells that had been treated with ACR and/or SCGB3A2 were washed in the annexin V binding buffer contained in the kit. The cells were incubated in annexin V binding buffer containing FITC-conjugated annexin V (20 μg/ml) and propidium iodide (PI) (50 μg/ml) for 15 min in the dark to detect dead cells. Cell nuclei were incubated in T-PBS for 15 min at RT and then both dead and living cells were stained with 300 nM DAPI for 5 min in the dark at RT. Cells were fixed with 4% PFA in PB for 15 min at RT, washed in PBS 3 times, and then mounted with CC/Mount™. Externalized phosphatidylserine was visualized with FITC-conjugated annexin V and detected with an FV10i-LIV confocal laser scanning biological microscope (Olympus). The TUNEL-positive rate

(%) was determined by counting TUNEL-positive cells and all nuclei in 5 randomly chosen fields within each well. The annexin V binding rate (%) was determined by counting the cells double-positive for annexin V and PI, and all nuclei stained with DAPI in 5 randomly chosen fields within each well. Experiments were repeated more than 4 times.

Detection of ROS

Cells treated with ACR and/or SCGB3A2 were incubated in DMEM containing 5 μM CellROX Green Reagent (Life Technologies, Carlsbad, CA, USA) for 1 hr at 37°C in the dark. Cells were then fixed with 4% PFA in PB at RT for 15 min. Cells were incubated with 300 nM DAPI for 5 min in the dark and then mounted with CC/Mount™. Cells were washed in PBS three times between each step. The green fluorescence signals were detected with the FV10i-LIV confocal laser scanning biological microscope. The fluorescence intensity was determined by using software installed on the FV 10i-LIV confocal laser scanning biological microscope in 5 randomly chosen fields within each well. Experiments were repeated more than 3 times.

Detection of p53 and phosphorylated p53

Immunocytochemistry using anti-p53 and anti-p-p53 antibody (Cell Signaling Technology, Danvers, MA, USA) was performed to detect p53 and phosphorylated p53 [p-p53 (Ser 18)], respectively. In brief, cells treated with ACR and/or SCGB3A2 were fixed with 4% PFA in PB for 15 min at RT. Cells were incubated in T-PBS for 15 min at RT and then in 3% BSA in PBS for 1 hr at RT. Cells were incubated with anti-p53 or anti-p-p53 antibody overnight at 4°C, followed by Alexa Fluor 488-conjugated goat anti-mouse IgG or Alexa Fluor 488-conjugated donkey anti-rabbit IgG (Life Technologies), respectively for 30 min at RT in the dark. Nuclei were stained by incubation with 300 nM DAPI and cells were mounted with CC/Mount™. Fluorescent signals were observed using the FV10i-LIVconfocal laser scanning biological microscope. Cells positive for p53, p-p53, and DAPI were counted in 5 randomly chosen fields within each well. Experiments were repeated more than 6 times.

Immunoblotting was performed as described by Kurotani *et al.* [21] using the above-mentioned antibodies and anti-β-actin antibody (Sigma-Aldrich, Missouri, USA). All immunoreactive bands were visualized using Immuno-Star LD (WAKO, Osaka, Japan) or ECL (GE Healthcare, Buckinghamshire, UK) chemiluminescence reagents with a MicroChemi (Bio-Imaging Systems, Jerusalem, Israel) imaging system. The density of immunoreactive bands was analyzed using the Image J software. Experiments were repeated more than 6 times.

Statistical analysis

Values for ROS detection, immunocytochemistry, and immunoblotting are expressed as mean±SEM. Statistical analyses of the results of the TUNEL and annexin V binding assays were performed using the chi-square test. Results of the ROS detection and the detection of p53- and p-p53-positive cells were analyzed using Student's *t*-test. Differences resulting in P values <0.05 were considered statistically significant.

III. Results

Decrease in ACR-induced apoptosis by SCGB3A2

The TUNEL assay and the annexin V binding assay were performed to detect ACR-induced apoptosis. The number of TUNEL-positive cells increased by ACR (Fig. 1A-b, e, h) compared with that of control cells (Fig. 1A-a, d, g). Annexin V-bound cells, indicative of apoptosis, were observed to have a decrease in apoptotic volume with strong green fluorescent signals in ACR-stimulated cells (Fig. 1C-a); these signals were decreased by SCGB3A2 (Fig. 1C-b). The number of Annexin V-bound cells was also increased by ACR, compared with control cells (Fig. 1D). ACR-induced apoptosis was markedly decreased by SCGB3A2 (Fig. 1A-c, f, i, C, D). Apoptosis was induced by ACR in a dose-dependent manner, and SCGB3A2 reduced ACR-induced apoptosis at all doses examined (Fig. 1B, D).

Effect of SCGB3A2 on ACR-induced production of ROS

ROS levels were measured to evaluate the effect of SCGB3A2 on ACR-induced production of ROS. There was almost no production of ROS in healthy cells (Fig. 2A-a, d, g, j). Exposure to ACR induced the production of ROS, as expected (Fig. 2A-b, e, h, k), and the increase in ROS was ACR dose-dependent (Fig. 2B). The ACR-induced production of ROS was not significantly decreased by SCGB3A2 at any concentration of ACR used (Fig. 2A-i, l, B).

Decrease in p53 phosphorylation by SCGB3A2

Immunocytochemistry and immunoblotting for phosphorylated p53 (p-p53 (Ser 18)) and whole p53 were performed to determine whether p53 phosphorylation (Ser 18) was altered by ACR and/or SCGB3A2. In these experiments, cells were stimulated by treatment with 15 μM ACR. The number of cells expressing p-p53 (Ser 18) increased by ACR (Fig. 3A-b, e, h, k) compared with that of control cells (Fig. 3A-a, d, g, j). This effect was significantly decreased by SCGB3A2 (Fig. 3A-c, f, i, l) compared with the ACR-stimulated cells (Fig. 3A-b, e, h, k). The percentage of p-p53 (Ser 18)-expressing cells stimulated by ACR was significantly decreased by SCGB3A2 (Fig. 3C). On the other hand, the number of cells expressing whole p53 was similar under all conditions (Fig. 3B), and regardless of treatment with ACR and/or SCGB3A2 (Fig. 3D).

The presence of p-p53 (Ser 18), determined by immunoblotting, was drastically increased by ACR, and this phosphorylation was significantly decreased by SCGB3A2 (Fig. 3E). The immunoreactive level of p-p53 (Ser18) was decreased to about 37% in the presence of SCGB3A2 com-

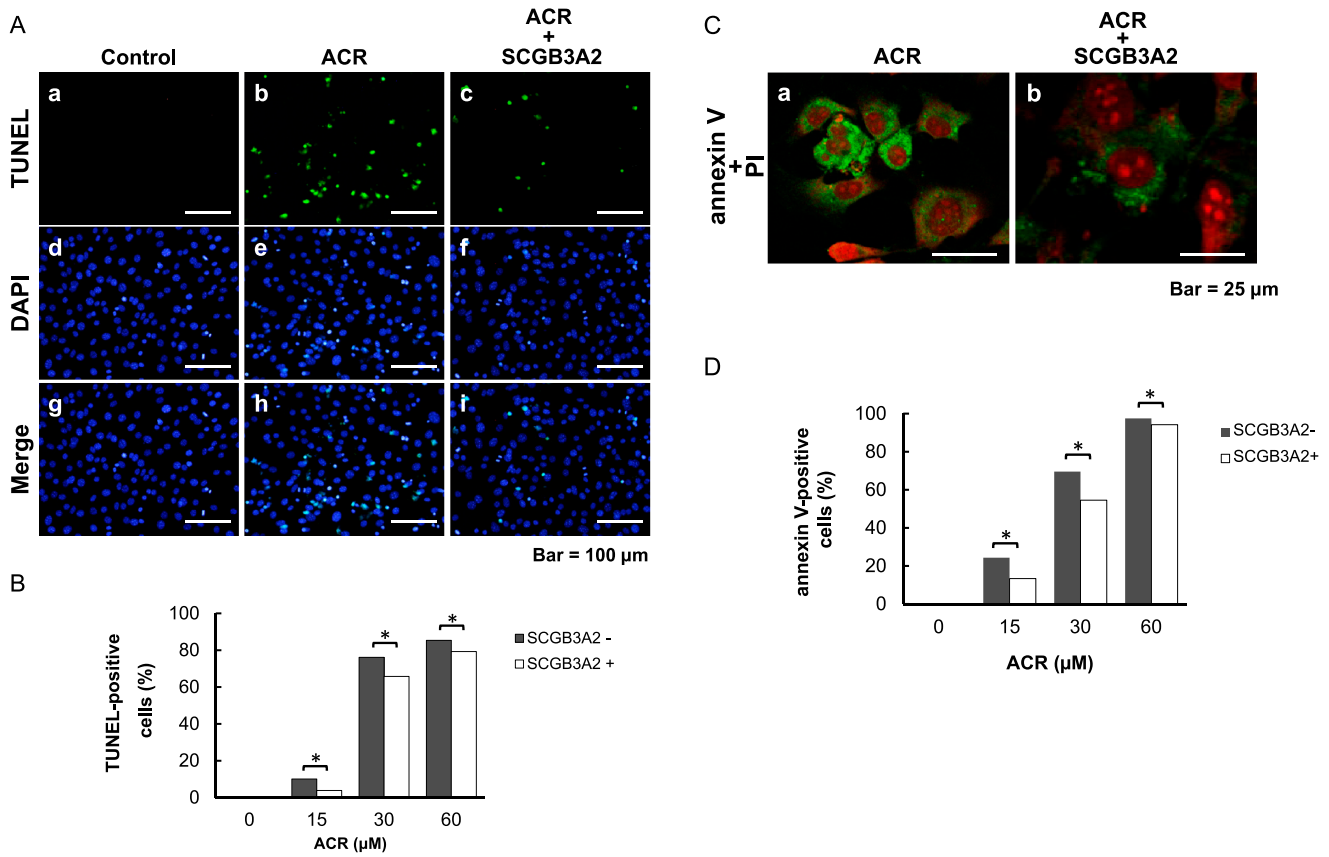

Fig. 1. SCGB3A2 decreases ACR-induced apoptosis. **A**. Images from the TUNEL assay and nuclear staining. TUNEL-positive cells were stained with green fluorescence (**a–c**) and nuclei were stained with blue fluorescence using DAPI (**d–f**). Merged images are shown in the lowest panel (**g–i**). No TUNEL-positive cells were observed in the control cells with (data not shown) or without SCGB3A2 (**a** and **g**). The number of TUNEL-positive cells was increased by ACR stimulation (**b** and **h**). The number of TUNEL-positive cells increased by ACR was decreased by SCGB3A2 (**c** and **i**). Representative images with or without 15 μM ACR stimulation are shown. Bar=100 μm. **B**. Effect of ACR on the TUNEL-positive rate. The rate is expressed as the percentage of TUNEL-positive cells within the cell population. **P*<0.05 between ACR-exposed cells with and without SCGB3A2 (n=4). **C**. Images from the annexin V binding assay and nuclear staining. Annexin V-positive cells were visualized with green fluorescence using FITC-conjugated annexin V; the nuclei of dead cells were stained with red fluorescence using PI; and then the signals were merged (**a** and **b**). All nuclei were stained by DAPI (data not shown). No annexin V-positive cells were observed in control cells with or without SCGB3A2 (data not shown). Representative images from experiments with 15 μM ACR stimulation in the absence or presence of SCGB3A2 are shown. Bar=25 μm. **D**. Effect of ACR concentration on the annexin V-positive rate. The rate is expressed as the percentage of annexin V and PI double-positive cells within the cell population. **P*<0.05 comparing ACR-exposed cells with and without SCGB3A2 (n=6).

pared with the immunoreactive level of p-p53 (Ser18) in the absence of SCGB3A2 (Fig. 3F). The immunoreactive bands for whole p53 and β-actin were not changed under any conditions (Fig. 3E and F).

IV. Discussion

This study revealed a new role for SCGB3A2 as an anti-apoptotic agent in experimental ACR exposure, using the mouse normal lung fibroblast cell line MLg. SCGB3A2 is known to be an anti-inflammatory cytokine-like protein [9] with growth factor [22] and antifibrotic [23] activities. Because ACR contained in cigarette smoke is considered to be the most important risk factor for COPD [4, 32], SCGB3A2 may potentially be used as a tool to improve COPD.

A COPD model mouse has been established by the use of ACR [7] or smoking [12, 30]. ACR has also been used to create cell death models in various cell lines [31, 34, 47, 50]. The mechanism of ACR-induced cell death, including apoptosis, has been studied in the human alveolar adenocarcinoma cell line A549 [42]. Apoptosis in lung structural cells, such as alveolar epithelial and endothelial cells, is assumed to be an important upstream event in the pathogenesis of COPD [13]. In the present study, apoptosis of MLg cells was induced by ACR stimulation. The ratio of apoptotic cells was significantly decreased by SCGB3A2 in the presence of various concentrations of ACR (15, 30, and 60 μM), showing that SCGB3A2 suppressed ACR-induced apoptosis. In particular, SCGB3A2 markedly decreased the apoptosis ratio in the presence of 15 μM ACR. Since ACR was shown to induce cell death through the production of ROS and phosphorylation of p53 using the A549 cell line [42], we investigated the effect of SCGB3A2 on ACR-

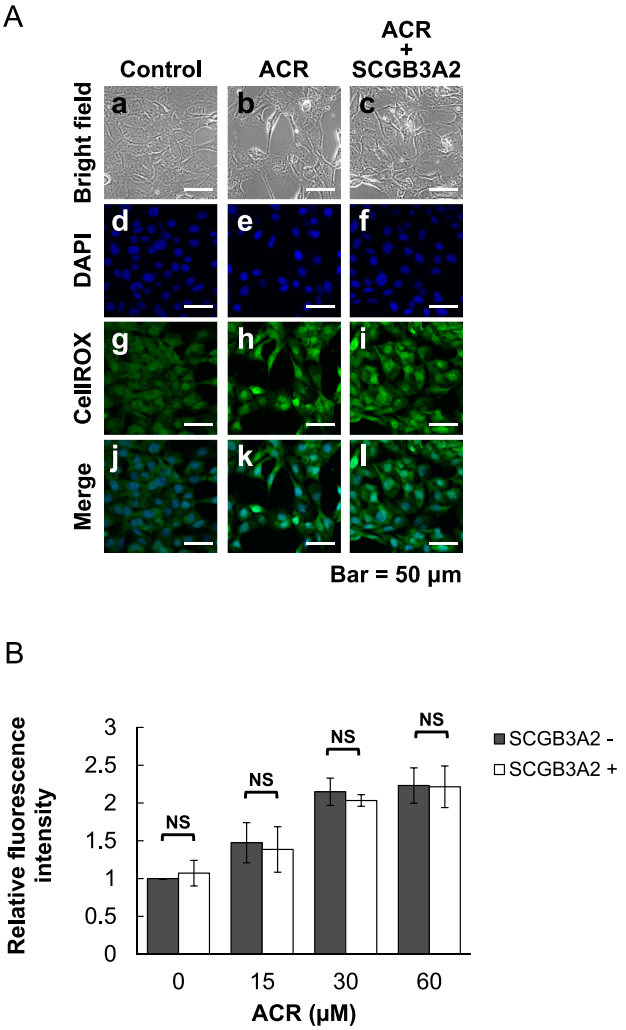

Fig. 2. Effect of SCGB3A2 on ACR-induced production of ROS. **A**. Images from the detection of ROS and nuclear staining. The production of ROS, visualized using CellROX Green Reagent (green signal, **g–i**), was increased by ACR (**h** and **k**). The ACR-induced production of ROS was not changed by SCGB3A2 (**i** and **l**). No green fluorescence signals for ROS were observed in control cells with (data not shown) or without (**g**) SCGB3A2. Cell morphology was observed by using a phase-contrast microscope (**a–c**); the nuclei were stained with DAPI (**d–f**). The green fluorescence signals for ROS and blue fluorescence signals for nuclei were merged (**j–l**). Representative images with or without 15 μM ACR stimulation are shown. Bar=50 μm. **B**. Effect of ACR concentration on the production of ROS. Data shown are the average of three independent experiments (n=3).

induced ROS production and phosphorylation of p53. ROS was increased by ACR in a dose-dependent manner, but ROS production was not affected by SCGB3A2. This was unexpected because our previous DNA microarray studies using lungs of mice that were treated with or without SCGB3A2 for 12 hr, demonstrated that the expression of genes involved in "repression of ROS producing systems" were up-regulated by SCGB3A2 [22]. ACR has been found to induce the generation of ROS, such as superoxide anion ($-O_2^-$) and hydroxyl radical (–OH), and to initiate lipid peroxidation [1, 39]. Inside the cell, the superoxide anion is converted to hydrogen peroxide (H_2O_2) and oxygen (O_2) by superoxide dismutase (SOD), and the resulting H_2O_2 is converted into H_2O and O_2 by catalase (CAT) and glutathione peroxidase (GPX) [28]. Our previous DNA microarray study [22] showed that SCGB3A2 increased expression of SOD3 and GPX3. However, SOD3 is predominantly found in the extracellular matrix of mammalian tissues [27, 38] and GPX3 is secreted into the extracellular fluid and present in plasma and serum [43]. Thus, it is conceivable that ACR-induced production of ROS is not suppressed by SCGB3A2.

The effect of SCGB3A2 on the phosphorylation of p53 was investigated in the presence of 15 μM ACR and/or SCGB3A2 by using immunocytochemistry and immunoblotting. The level of p-p53 was increased by ACR, and significantly decreased by SCGB3A2, as determined by using immunocytochemistry. On the other hand, the number of whole p53-expressing cells was not changed under any conditions, as determined using immunocytochemistry. By immunoblotting, the immunoreactive bands for p-p53 were markedly increased by ACR and decreased to control

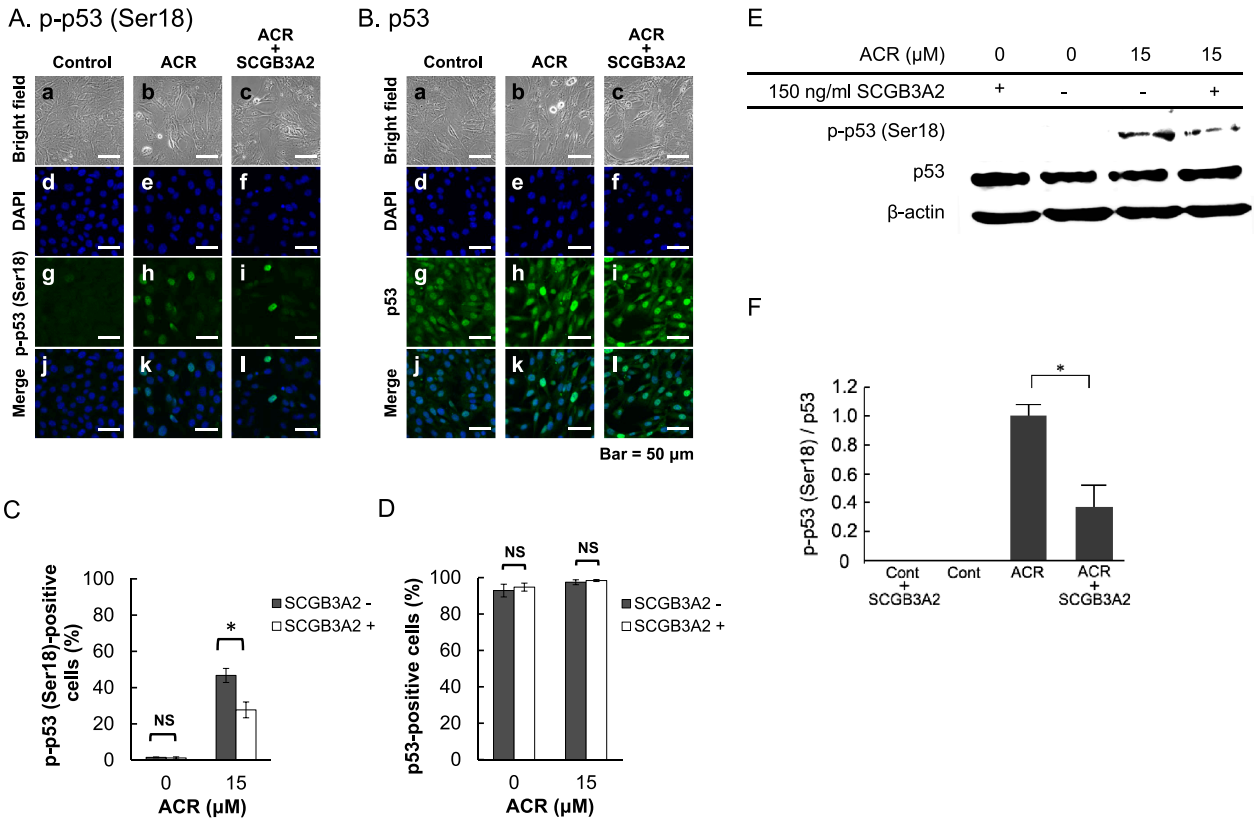

Fig. 3. Effect of SCGB3A2 on phosphorylation of p53. **A**. Images of phosphorylated p53 (p-p53) and nuclear staining. The level of p53 phosphorylation (on Ser 18) induced by ACR (**h** and **k**) was decreased by SCGB3A2 (**i** and **l**). Cell morphology was observed using a phase-contrast microscope (**a–c**), and nuclei were stained with DAPI (**d–f**). p-p53 (Ser 18) was visualized as green fluorescence signals within the nuclei (**h** and **i**). No green fluorescence signals for p-p53 were observed in control cells with (data not shown) or without (**g**) SCGB3A2. The green fluorescence signals for p-p53 (Ser 18) and blue fluorescence signals for nuclei were merged (**j–l**). Representative images with and without 15 μM ACR stimulation are shown (n=5). Bar=50 μm. **B**. Images of whole p53 and nuclear staining. The expression of whole p53 was not changed under any conditions: control with (data not shown) and without SCGB3A2 (**g**), 15 μM ACR stimulation (**h**), ACR stimulation in the presence of SCGB3A2 (**i**). Cell morphology was observed using a phase-contrast microscope (**a–c**) and nuclei were stained with DAPI (**d–f**). p53 was visualized as green fluorescence signals in nuclei (**g–i**). The green fluorescence signals for p53 and blue fluorescence signals for nuclei were merged (**j–l**). Representative images with 15 μM ACR stimulation are shown (n=5). Bar=50 μm. **C**. Effect of ACR on the p53 (Ser 18)-positive cell rate. The rate is expressed as the percentage of p53 (Ser 18)-positive cells in the cell population. Data shown are the average of five independent experiments (n=5). **P*<0.05. **D**. Effect of ACR on the whole p53-positive cells rate. The rate is expressed as the percentage of whole p53-positive cells within the cell population. Data shown are the average of five independent experiments (n=5). NS: not significant. **E**. Immunoblotting for p-p53 (Ser 18), whole p53, and β-actin. Phosphorylation of p53 was increased by ACR (15 μM). The intensity of the p-p53 (Ser 18)-specific band was decreased by SCGB3A2 (150 ng/ml). No immunopositive bands for p-p53 (Ser 18) were detected in control cells with or without SCGB3A2. The immunopositive bands for whole p53 and β-actin were not changed under any conditions. The image of a representative immunoblot is shown. More than six independent experiments were carried out, and similar results were obtained. **F**. The ratio of p-p53 (Ser 18) per whole p53. The presence of SCGB3A2 reduced the immunopositive density for p-p53 (Se 18) in ACR-treated cells to 37% of its value in the absence of SCGB3A2. Data shown are the average of six independent experiments (n=6). **P*<0.05.

levels in the presence of SCGB3A2. The immunoreactive bands for whole p53 and β-actin were detected at similar levels in all conditions. These results demonstrate that SCGB3A2 inhibits the p53 phosphorylation induced by ACR. The serine residue at codon 15 of human p53 (equivalent to Ser 18 of murine p53) is phosphorylated by activation of ataxia telangiectasia mutated (ATM), ataxia telangiectasia and Rad3-related protein (ATR), and DNA-activated protein kinase (DNA-PK), all of which are members of the phosphoinositide 3-kinase family [8, 45, 48]. In addition, extracellular signal-regulated kinase (ERK) and p38 MAPK have a direct role in the UVB-induced phosphorylation of p53 at Ser 15 *in vivo* [44]. It was also reported that protein phosphatase-2A (PP2A) directly dephosphorylates human p53 (Ser 15) *in vitro* and *in vivo* [40]. Based on this information, it is possible that SCGB3A2 may suppress the activities of ATM, ATR, DNA-PK, ERK, and/or p38 MAPK to phosphorylate p53 and/or facilitate the activation of PP2A. MARCO has been reported as a receptor for SCGB3A2 [5], however MARCO is not expressed in epithelial and fibroblastic cells, including MLg cells [22]. This data led us to suggest the presence of an SCGB3A2-specific receptor [22]. Since nobody has identified this receptor, the cell signaling pathway activated after the binding of SCGB3A2 to the receptor is still unknown. Further studies are required to address these

questions.

In conclusion, this study demonstrated that SCGB3A2 inhibits ACR-induced apoptosis in MLg cells, in part through decreased phosphorylation of p53.

V. Acknowledgments

We thank Mr. Yoshimasa Watanabe (Yamagata University) for technical support. This study was supported by a Grant-in-Aid for Young Scientists (C) from the Naito Foundation Subsidy for Female Researchers after Maternity Leave, and by the Dissemination of Tenure Tracking System Program of the Ministry of Education, Culture, Sports, Science and Technology-Japan.

VI. References

1. Adams, J. D. Jr. and Klaidman, L. K. (1993) Acrolein-induced oxygen radical formation. *Free Radic. Biol. Med.* 15; 187–193.
2. Akinci, A. C. and Yildirim, E. (2013) Factors affecting health status in patients with chronic obstructive pulmonary disease. *Int. J. Nurs. Pract.* 19; 31–38.
3. Barnes, P. J., Shapiro, S. D. and Pauwels, R. A. (2003) Chronic obstructive pulmonary disease: molecular and cellular mechanisms. *Eur. Respir. J.* 22; 672–688.
4. Bein, K. and Leikauf, G. D. (2011) Acrolein—a pulmonary hazard. *Mol. Nutr. Food Res.* 55; 1342–1360.
5. Bin, L. H., Nielson, L. D., Liu, X., Mason, R. J. and Shu, H. B. (2003) Identification of uteroglobin-related protein 1 and macrophage scavenger receptor with collagenous structure as a lung-specific ligand-receptor pair. *J. Immunol.* 171; 924–930.
6. Borchers, M. T., Wesselkamper, S., Wert, S. E., Shapiro, S. D. and Leikauf, G. D. (1999) Monocyte inflammation augments acrolein-induced Muc5ac expression in mouse lung. *Am. J. Physiol.* 277; L489–497.
7. Borchers, M. T., Wesselkamper, S. C., Harris, N. L., Deshmukh, H., Beckman, E., Vitucci, M., Tichelaar, J. W. and Leikauf, G. D. (2007) Cd8+ T cells contribute to macrophage accumulation and airspace enlargement following repeated irritant exposure. *Exp. Mol. Pathol.* 83; 301–310.
8. Canman, C. E., Lim, D. S., Cimprich, K. A., Taya, Y., Tamai, K., Sakaguchi, K., Appella, E., Kastan, M. B. and Siliciano, J. D. (1998) Activation of the ATM kinase by ionizing radiation and phosphorylation of p53. *Science* 281; 1677–1679.
9. Chiba, Y., Kurotani, R., Kusakabe, T., Miura, T., Link, B. W., Misawa, M. and Kimura, S. (2006) Uteroglobin-related protein 1 expression suppresses allergic airway inflammation in mice. *Am. J. Respir. Crit. Care Med.* 173; 958–964.
10. Cosio, M. G., Saetta, M. and Agusti, A. (2009) Immunologic aspects of chronic obstructive pulmonary disease. *N. Engl. J. Med.* 360; 2445–2454.
11. Costa, D. L., Kutzman, R. S., Lehmann, J. R. and Drew, R. T. (1986) Altered lung function and structure in the rat after subchronic exposure to acrolein. *Am. Rev. Respir. Dis.* 133; 286–291.
12. D'Hulst, A. I., Vermaelen, K. Y., Brusselle, G. G., Joos, G. F. and Pauwels, R. A. (2005) Time course of cigarette smoke-induced pulmonary inflammation in mice. *Eur. Respir. J.* 26; 204–213.
13. Demedts, I. K., Demoor, T., Bracke, K. R., Joos, G. F. and Brusselle, G. G. (2006) Role of apoptosis in the pathogenesis of COPD and pulmonary emphysema. *Respir. Res.* 7; 53.
14. Deshmukh, H. S., Case, L. M., Wesselkamper, S. C., Borchers, M. T., Martin, L. D., Shertzer, H. G., Nadel, J. A. and Leikauf, G. D. (2005) Metalloproteinases mediate mucin 5AC expression by epidermal growth factor receptor activation. *Am. J. Respir. Crit. Care Med.* 171; 305–314.
15. Deshmukh, H. S., McLachlan, A., Atkinson, J. J., Hardie, W. D., Korfhagen, T. R., Dietsch, M., Liu, Y., Di, P. Y., Wesselkamper, S. C., Borchers, M. T. and Leikauf, G. D. (2009) Matrix metalloproteinase-14 mediates a phenotypic shift in the airways to increase mucin production. *Am. J. Respir. Crit. Care Med.* 180; 834–845.
16. Dostert, C., Petrilli, V., Van Bruggen, R., Steele, C., Mossman, B. T. and Tschopp, J. (2008) Innate immune activation through Nalp3 inflammasome sensing of asbestos and silica. *Science* 320; 674–677.
17. Garcia-Polo, C., Alcazar-Navarrete, B., Ruiz-Iturriaga, L. A., Herrejon, A., Ros-Lucas, J. A., Garcia-Sidro, P., Tirado-Conde, G., Lopez-Campos, J. L., Martinez-Rivera, C., Costan-Galicia, J., Mayoralas-Alises, S., De Miguel-Diez, J. and Miravitlles, M. (2012) Factors associated with high healthcare resource utilisation among COPD patients. *Respir. Med.* 106; 1734–1742.
18. Hogg, J. C., Chu, F., Utokaparch, S., Woods, R., Elliott, W. M., Buzatu, L., Cherniack, R. M., Rogers, R. M., Sciurba, F. C., Coxson, H. O. and Pare, P. D. (2004) The nature of small-airway obstruction in chronic obstructive pulmonary disease. *N. Engl. J. Med.* 350; 2645–2653.
19. Kim, C. E., Lee, S. J., Seo, K. W., Park, H. M., Yun, J. W., Bae, J. U., Bae, S. S. and Kim, C. D. (2010) Acrolein increases 5-lipoxygenase expression in murine macrophages through activation of ERK pathway. *Toxicol. Appl. Pharmacol.* 245; 76–82.
20. Klug, J., Beier, H. M., Bernard, A., Chilton, B. S., Fleming, T. P., Lehrer, R. I., Miele, L., Pattabiraman, N. and Singh, G. (2000) Uteroglobin/Clara cell 10-kDa family of proteins: nomenclature committee report. *Ann. N Y Acad. Sci.* 923; 348–354.
21. Kurotani, R., Tahara, S., Sanno, N., Teramoto, A., Mellon, P. L., Inoue, K., Yoshimura, S. and Osamura, R. Y. (1999) Expression of Ptx1 in the adult rat pituitary glands and pituitary cell lines: hormone-secreting cells and folliculo-stellate cells. *Cell Tissue Res.* 298; 55–61.
22. Kurotani, R., Tomita, T., Yang, Q., Carlson, B. A., Chen, C. and Kimura, S. (2008) Role of secretoglobin 3A2 in lung development. *Am. J. Respir. Crit. Care Med.* 178; 389–398.
23. Kurotani, R., Okumura, S., Matsubara, T., Yokoyama, U., Buckley, J. R., Tomita, T., Kezuka, K., Nagano, T., Esposito, D., Taylor, T. E., Gillette, W. K., Ishikawa, Y., Abe, H., Ward, J. M. and Kimura, S. (2011) Secretoglobin 3A2 suppresses bleomycin-induced pulmonary fibrosis by transforming growth factor beta signaling down-regulation. *J. Biol. Chem.* 286; 19682–19692.
24. Lemaitre, V., Dabo, A. J. and D'Armiento, J. (2011) Cigarette smoke components induce matrix metalloproteinase-1 in aortic endothelial cells through inhibition of mTOR signaling. *Toxicol. Sci.* 123; 542–549.
25. Lubin, R., Zalcman, G., Bouchet, L., Tredanel, J., Legros, Y., Cazals, D., Hirsch, A. and Soussi, T. (1995) Serum p53 antibodies as early markers of lung cancer. *Nat. Med.* 1; 701–702.
26. MacNee, W. (2005) Pathogenesis of chronic obstructive pulmonary disease. *Proc. Am. Thorac. Soc.* 2; 258–266.
27. Marklund, S. L. (1984) Extracellular superoxide dismutase in human tissues and human cell lines. *J. Clin. Invest.* 74; 1398–1403.
28. Mates, J. M., Perez-Gomez, C. and Nunez de Castro, I. (1999) Antioxidant enzymes and human diseases. *Clin. Biochem.* 32; 595–603.
29. Mattioni, M., Chinzari, P., Soddu, S., Strigari, L., Cilenti, V. and Mastropasqua, E. (2013) Serum p53 antibody detection in patients with impaired lung function. *BMC Cancer* 13; 62.

30. Meshi, B., Vitalis, T. Z., Ionescu, D., Elliott, W. M., Liu, C., Wang, X. D., Hayashi, S. and Hogg, J. C. (2002) Emphysematous lung destruction by cigarette smoke. The effects of latent adenoviral infection on the lung inflammatory response. *Am. J. Respir. Cell Mol. Biol.* 26; 52–57.
31. Mohammad, M. K., Avila, D., Zhang, J., Barve, S., Arteel, G., McClain, C. and Joshi-Barve, S. (2012) Acrolein cytotoxicity in hepatocytes involves endoplasmic reticulum stress, mitochondrial dysfunction and oxidative stress. *Toxicol. Appl. Pharmacol.* 265; 73–82.
32. Moretto, N., Volpi, G., Pastore, F. and Facchinetti, F. (2012) Acrolein effects in pulmonary cells: relevance to chronic obstructive pulmonary disease. *Ann. N Y Acad. Sci.* 1259; 39–46.
33. Nagai, K., Betsuyaku, T., Kondo, T., Nasuhara, Y. and Nishimura, M. (2006) Long term smoking with age builds up excessive oxidative stress in bronchoalveolar lavage fluid. *Thorax* 61; 496–502.
34. Nardini, M., Finkelstein, E. I., Reddy, S., Valacchi, G., Traber, M., Cross, C. E. and van der Vliet, A. (2002) Acrolein-induced cytotoxicity in cultured human bronchial epithelial cells. Modulation by alpha-tocopherol and ascorbic acid. *Toxicology* 170; 173–185.
35. Niimi, T., Keck-Waggoner, C. L., Popescu, N. C., Zhou, Y., Levitt, R. C. and Kimura, S. (2001) UGRP1, a uteroglobin/Clara cell secretory protein-related protein, is a novel lung-enriched downstream target gene for the T/EBP/NKX2.1 homeodomain transcription factor. *Mol. Endocrinol.* 15; 2021–2036.
36. Niimi, T., Kurotani, R., Kimura, S. and Kitagawa, Y. (2006) Identification and expression of alternative splice variants of the mouse Ppp1r3b gene in lung epithelial cells. *Biochem. Biophys. Res. Commun.* 349; 588–596.
37. Nishimura, S. and Zaher, C. (2004) Cost impact of COPD in Japan: opportunities and challenges? *Respirology* 9; 466–473.
38. Oury, T. D., Chang, L. Y., Marklund, S. L., Day, B. J. and Crapo, J. D. (1994) Immunocytochemical localization of extracellular superoxide dismutase in human lung. *Lab. Invest.* 70; 889–898.
39. Patel, J. M. (1987) Stimulation of cyclophosphamide-induced pulmonary microsomal lipid peroxidation by oxygen. *Toxicology* 45; 79–91.
40. Qin, J., Chen, H. G., Yan, Q., Deng, M., Liu, J., Doerge, S., Ma, W., Dong, Z. and Li, D. W. (2008) Protein phosphatase-2A is a target of epigallocatechin-3-gallate and modulates p53-Bak apoptotic pathway. *Cancer Res.* 68; 4150–4162.
41. Rabe, K. F., Hurd, S., Anzueto, A., Barnes, P. J., Buist, S. A., Calverley, P., Fukuchi, Y., Jenkins, C., Rodriguez-Roisin, R., van Weel, C. and Zielinski, J. (2007) Global strategy for the diagnosis, management, and prevention of chronic obstructive pulmonary disease: gold executive summary. *Am. J. Respir. Crit. Care Med.* 176; 532–555.
42. Roy, J., Pallepati, P., Bettaieb, A. and Averill-Bates, D. A. (2010) Acrolein induces apoptosis through the death receptor pathway in A549 lung cells: role of p53. *Can. J. Physiol. Pharmacol.* 88; 353–368.
43. Rush, J. W. and Sandiford, S. D. (2003) Plasma glutathione peroxidase in healthy young adults: influence of gender and physical activity. *Clin. Biochem.* 36; 345–351.
44. She, Q. B., Chen, N. and Dong, Z. (2000) ERKs and p38 kinase phosphorylate p53 protein at serine 15 in response to UV radiation. *J. Biol. Chem.* 275; 20444–20449.
45. Shieh, S. Y., Ikeda, M., Taya, Y. and Prives, C. (1997) DNA damage-induced phosphorylation of p53 alleviates inhibition by MDM2. *Cell* 91; 325–334.
46. Siganaki, M., Koutsopoulos, A. V., Neofytou, E., Vlachaki, E., Psarrou, M., Soulitzis, N., Pentilas, N., Schiza, S., Siafakas, N. M. and Tzortzaki, E. G. (2010) Deregulation of apoptosis mediators' p53 and bcl2 in lung tissue of COPD patients. *Respir. Res.* 11; 46.
47. Tanel, A. and Averill-Bates, D. A. (2007) Activation of the death receptor pathway of apoptosis by the aldehyde acrolein. *Free Radic. Biol. Med.* 42; 798–810.
48. Tibbetts, R. S., Brumbaugh, K. M., Williams, J. M., Sarkaria, J. N., Cliby, W. A., Shieh, S. Y., Taya, Y., Prives, C. and Abraham, R. T. (1999) A role for ATR in the DNA damage-induced phosphorylation of p53. *Genes Dev.* 13; 152–157.
49. Vijayan, V. K. (2013) Chronic obstructive pulmonary disease. *Indian J. Med. Res.* 137; 251–269.
50. Yang, E. S., Woo, S. M., Choi, K. S. and Kwon, T. K. (2011) Acrolein sensitizes human renal cancer Caki cells to TRAIL-induced apoptosis via ROS-mediated up-regulation of death receptor-5 (DR5) and down-regulation of Bcl-2. *Exp. Cell Res.* 317; 2592–2601.